bioRχiv
THE PREPRINT SERVER FOR BIOLOGY

ARTICLE PREPRINT

Estrogen Drives Melanocortin Neurons To Reduce Sedentary Behavior

William C. Krause[1], Ruben Rodriguez[1], Bruno Gegenhuber[2], Navneet Matharu[3], Andreas N. Rodriguez[1], Adriana M. Padilla[4], Candice B. Herber[1], Stephanie M. Correa[1,5], Nadav Ahituv[3], Jessica Tollkuhn[6], and Holly A. Ingraham[1]

Estrogen depletion in both rodents and humans leads to inactivity, unhealthy fat accumulation, and metabolic syndrome[1], underscoring the conserved metabolic benefits of estrogen signaling that inevitably decline with aging. Here, we uncover a hypothalamic node that integrates estrogen and melanocortin-4 receptor (MC4R) signaling to drive episodic bursts in activity prior to ovulation. Skirting the estrogen-dependent gating of this node reduces sedentary behavior long-term in both males and females. Our findings expand the impact of MC4R signaling beyond food intake regulation and rationalize reported sex-differences in melanocortin signaling including increased disease severity for women with MC4R-insuffciency. This newly identified hormone-dependent activity node illustrates the potency of estrogen in maintaining an active lifestyle.

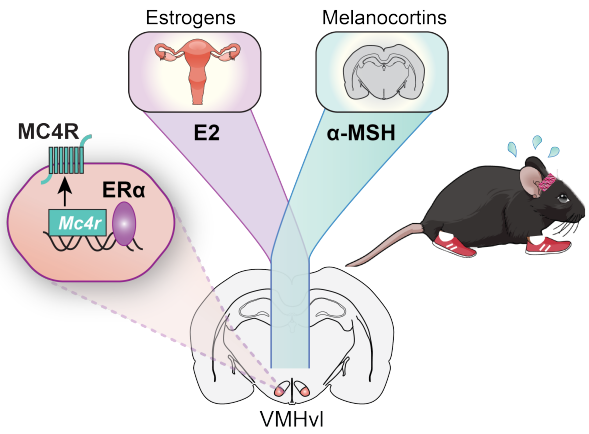

Rodent studies show that central estrogen receptor alpha (ERα) activation by 17β-estradiol (E2) relaxes homeostatic constraints to satisfy the energetic demands of reproduction, temporarily allowing energy expenditure to outpace energy intake[2]. Thus, surges in estrogen override normal homeostatic feedback to simultaneously attenuate food intake and increase activity[3-7]. To address how estrogen resets energy homeostasis, we focused on ERα signaling in the ventrolateral ventromedial hypothalamic nucleus (VMHvl) as a major determinant of female energy expenditure. We identify melanocortin-4 receptor (MC4R), which when mutated leads to human obesity[8], as a direct ERα target that is upregulated in a small subset of VMHvl^{ERα} neurons during proestrus or with E2. Restoring MC4R signaling in the VMHvl of *Mc4r*$^{-/-}$ null mice counteracts weight gain and drives physical activity in females despite their profound hyperphagia[9]. Bypassing E2-dependency in this node by chemogenetic stimulation or by CRISPR-mediated activation (CRISPRa) to raise *Mc4r* dosage increases physical activity in both sexes. Notably, CRISPRa manipulation engages this activity circuit long-term to reduce sedentary behavior, providing an opportunity to explore the benefits of sustained physical activity.

To identify the pathways and precise neuronal subset that prioritize energy utilization over storage, we asked if maximal physical activity depends solely on ERα signaling in the adult VMHvl. ERα was ablated in the VMHvl or in the arcuate (ARC) of adult female mice using stereotaxic delivery of AAV-Cre-GFP (VMHvl^{ERαKO}, ARC^{ERαKO}, **Fig. 1a**). Control female littermates received similarly targeted AAV-GFP injections (VMHvl^{Control} or ARC^{Control}). Reduced ambulatory activity was observed in VMHvl^{ERαKO}, but not in ARC^{ERαKO} females during the dark cycle with a mild reduction in thermogenic energy expenditure that corresponded to increased body weight over the course of 12 weeks post-AAV injection (**Fig. 1b and Extended Data Fig 1.1**). No changes in daily food intake were noted in either VMHvl^{ERαKO} or ARC^{ERαKO} cohorts (**Fig 1b**). This latter result points to the hindbrain nucleus of the solitary tract[10], rather than the ARC[7,11] for eliciting the major anorexigenic effects of estrogen. Alternatively, compensatory mechanisms might mask hyperphagia in ARC^{ERαKO} females. Ablating ERα in the ARC did lead to a surprisingly high bone mass phenotype[4]. When considered with other Cre-based genetic ERα knockout models, we conclude that ERα in the VMHvl is an essential driver of maximal physical activity in female mice.

1. Department of Cellular and Molecular Pharmacology School of Medicine, University of California, San Francisco, CA 94158. 2. Watson School of Biological Sciences, Cold Spring Harbor Labs, 3. Department of Bioengineering and Therapeutic Sciences and Institute for Human Genetics, University of California, San Francisco, CA 94158. 4. Graduate Program in Neuroscience, UCSF. 5. **Present Address:** Department of Integrative Biology and Physiology, University of California Los Angeles, Los Angeles, California 90095, USA. 6. Cold Spring Harbor Laboratory, Cold Spring Harbor, NY 11724. Co-corresponding Authors: tollkuhn@cshl.edu and holly.ingraham@ucsf.edu

VMHvl E2 signaling is reported to inhibit 5' AMP-activated kinase (AMPK)[5], which is known to inhibit the nutrient sensitive kinase, mTOR (mammalian target of rapamycin). Using ribosome phosphorylation as an established proxy for mTOR activity[12], we tested if pS6 might increase in female mice during proestrus (high E2) or with exogenous E2. A dramatic induction of pS6 signal was observed that localized to VMHvl^{ERα} neurons during proestrus or following estradiol benzoate (EB) injection into ovariectomized (OVX) females (**Fig. 1c, d**). Little to no pS6 signal was detected in the VMHvl^{ERα} of females during estrus (low E2), in females lacking ERα, or in intact males. (**Fig 1c and Extended Data Fig 1.2**), underscoring a complete dependence on E2 and ERα for this pS6 response. Induction of pS6 by EB in VMHvl^{ERα} neurons occurred slowly (>2 hrs post-hormone injection) pointing to a classical genomic response. In contrast to the VMHvl, no changes in pS6 induction were detected in adjacent ARC^{ERα} neurons (**Fig 1e**), demonstrating that VMHvl^{ERα} neurons are highly sensitive to E2 and exhibit a neuron type-specific response. Given that fasting and other cues for energy demand reduce pS6 (and mTOR) signaling[13], we suggest that estrogen and induction of pS6 in VMHvl^{ERα} neurons conveys the opposite to increase energy utilization.

Transcriptional profiling was then used to identify candidate signaling pathways that contribute to VMHvl E2-mediated activity. Among the 287 differentially expressed genes (DEGs), significantly enriched pathways included peptidergic signaling (R-MMU-375276), abnormal mammalian energy expenditure (MP: 0005450) and food intake (MP: 0005449) phenotypes (**Fig. 2a and Extended Data Table 1**). In particular, EB affected expression of several metabolically relevant neuropeptide receptors, including *Mc4r*, *Nmur2*, *Npy1r*, and *Ghsr*, as well as known estrogen and/or sex-dependent genes (*Cckar*, *Greb1*, *Pgr*[4,14]). Two of these receptors, MC4R[15,16] and NMUR2[17] affect locomotor behavior. Expression of *Mc4r* and *Nmur2* was induced by E2, and during proestrus (P), but was near absent during estrus (E) and in intact males (**Fig 2b, c and Extended Data Fig 2.1**). High-resolution mapping of ERα-chromatin interactions by CUT&RUN (Cleavage Under Targets and Release Using Nuclease)[18,19] demonstrated hormone-dependent ERα recruitment to the *Mc4r* promoter and to the *Nmur2* 3' UTR in mice treated with EB (**Fig 2d and Extended Data Fig 2.1**). Taken together, these data establish a direct molecular link between estrogen and MC4R signaling.

While *Mc4r* expression is reported in the VMH[20,21], little is known about its role in this brain region[22]. Using *Mc4r-t2a-Cre;Ai14*$^{fl/+}$ mice to mark MC4R neurons[23], we observed a complete concordance of *Mc4r* and ERα in the VMHvl. These VMHvl$^{ERα/MC4R}$ neurons represent ~40% of the broader VMHvl^{ERα} population (**Fig. 2e,f**). In contrast to the VMHvl, the medial amygdala (MEA) contains many more MEA^{MC4R} neurons lacking ERα. Induction of *Mc4r* in the MEA during

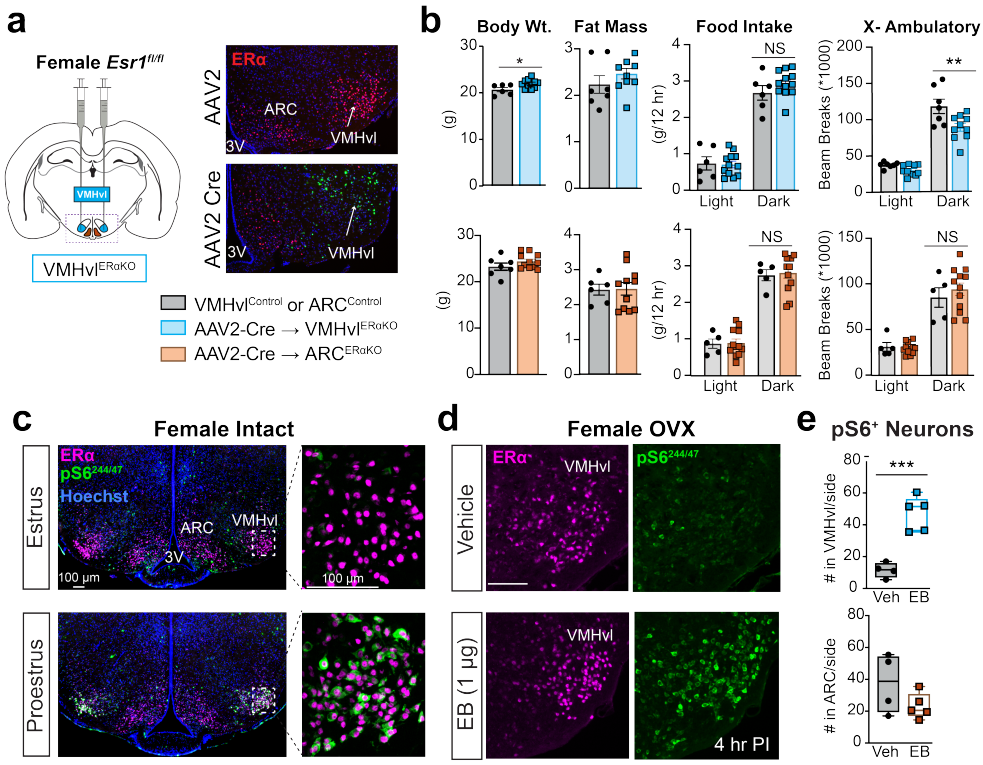

Fig. 1. VMHvl neurons maintain energy expenditure in adult females and are highly sensitive to estrogen. a, Control and spatially restricted ERα knockout mice were generated by stereotaxic delivery of AAV2-GFP or AAV2-Cre-GFP to the VMHvl or the ARC of *Esr1*$^{fl/fl}$ adult females. Successful hits were confirmed post-mortem by loss of ERα expression. **b**, Quantification of body weight, fat composition, food intake, and ambulatory activity in VMHvl^{ERαKO} (blue), ARC^{ERαKO} (orange), and their respective controls. VMHvl^{ERαKO} females were less active during the dark phase (RM 2-way ANOVA interaction effect $F_{(1,15)}$=4.548, P=0.0499, post hoc: P=0.0014) and heavier (unpaired 2-tailed t test $t_{(16)}$=2.365, P=0.0310) than controls. **c**, Increased ribosome phosphorylation (pS6$^{244/47}$, green) observed during proestrus localized to ERα neurons (magenta) in the VMHvl. **d**, Treatment of OVX female mice with estradiol benzoate (EB) significantly increased pS6 staining in VMHvl^{ERα} but not ARC^{ERα} neurons (unpaired 2-tailed t test: VMHvl $t_{(7)}$=6.074, P=0.0005; ARC $t_{(7)}$=1.562, P=0.1622).

proestrus is also substantially weaker (Fig 2g). No overlap was observed in two other regions of interest, including the paraventricular hypothalamus (PVH), a primary site that couples MC4R with its metabolic effects, and the lateral hypothalamic area (LHA) that harbors a small subset of LHA$^{MC3R/MC4R}$ neurons linked to increased locomotor activity[24]. Collectively, these data establish that *Mc4r* expression is tightly synchronized with the estrous cycle in a small subset of energy expenditure-promoting VMHvl female neurons.

Given the robust induction of *Mc4r* in the VMHvl by estrogen and the known sex-differences in *Mc4r* knockout/loss-of-function mutations in mice[16,25] and humans[26], we wished to know if the functional outputs of VMHvl^{MC4R} neurons were restricted to females. Initially, Cre-dependent expression of stimulatory DREADDs (hM3Dq) was used to activate VMHvl^{MC4R} neurons. Bilateral delivery of AAV-hM3Dq-mCherry into the VMHvl of both *Mc4r-t2a-Cre+* (Fig 3a) and Cre-negative littermates resulted in significant clozapine-n-oxide (CNO)-induced activity in DREADD-expressing VMHvl$^{MC4R::hM3Dq}$ females and males injected during the light cycle (ZT3-11), corresponding to their inactive period (Fig. 3b). Distance traveled 5 hrs post-CNO injection (PI) jumped significantly (~700-800%) in both sexes accompanied by a significant drop in sedentary behavior (Extended Data Fig 3.1); with total distance traveled in females exceeding that of males (~1.7 fold). Consistent with the minimal role of VMHvl in food intake, CNO failed to increase or decrease food consumption in the light and dark stages, respectively.

To determine if DREADD-dependent activity of VMHvl^{Mc4R} neurons was capable of producing weight loss in the face of overnutrition or high-fat diet (HFD), VMHvl$^{MC4R::hM3Dq}$ and VMHvl^{Cre-} control females were simultaneously fed HFD and chronically exposed to CNO in their drinking water (0.25 mg/mL) for 8 days. Stimulating VMHvl$^{MC4R::hM3Dq}$ neurons elicited a sustained increase in ambulatory activity (Extended Data Movie 3.2) and an initial precipitous drop in body weight of 12% (Fig 3e). Weight differences between experimental and control fe-

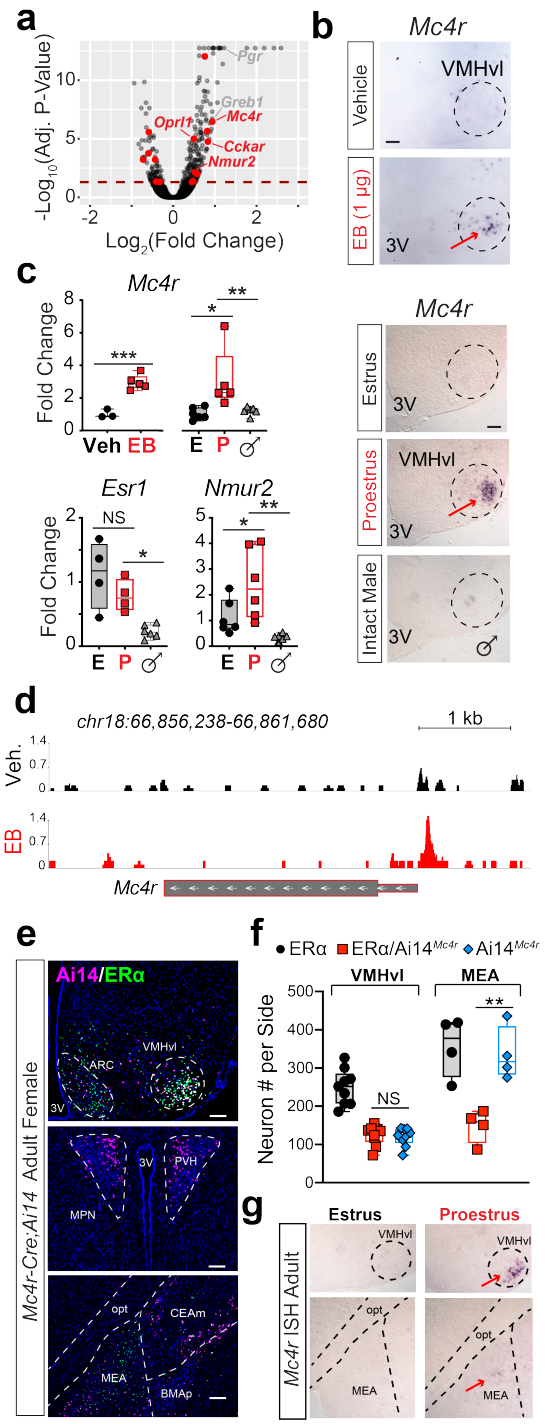

Figure 2. *Mc4r* is an estrogen-responsive gene in the VMHvl marking a distinct subset of VMHvl$^{ERa/MC4R}$ neurons. a, Transcriptional profiling of the VMHvl from vehicle and EB treated female mice identified 287 DEGs (Benjamini-Hochburg adjusted P<0.05), including a significantly enriched subset of peptidergic receptors (red). **b**, qPCR and ISH confirmed EB-dependent upregulation of *Mc4r* in the VMHvl (unpaired 2-tailed t test $t(6)$=6.519, P=0.0006). **c**, qPCR analysis of the indicated target genes in VMHvl isolated from estrus females (E), proestrus females (P), and males (♂) (1-way ANOVA: Mc4r $F_{(2,14)}$=6.428, P=0.0105, post hoc: E vs P P=0.0163 and P vs ♂ P=0.0189; Nmur2 $F_{(2,15)}$=8.469, P=0.0035, post hoc: E vs P P=0.0454 and P vs ♂ P=0.0030; Esr1 $F_{(2,11)}$=10.18, P=0.0031, post hoc: E vs ♂ P=0.0033 and P vs ♂ P=0.0374). **d,** CUT&RUN genome browser track showing EB-induced ERα binding at *Mc4r* promoter in sub-cortical brain regions collected from vehicle and EB (5 µg) treated gonadectomized mice. The summit of the peak corresponds with an ERE half-site. **e and f**, Images from *Ai14$^{Mc4r-t2a-Cre}$* female mice showing ERα (green) and Cre-dependent Ai14 (magenta) co-expression in the VMHvl, PVH, and MEA. In the VMHvl, nearly all Ai14^{Mc4r} neurons express ERα (unpaired 2-tailed t test, $t_{(16)}$=0.3669, P=0.7185). In the MEA, co-labeled neurons represent a fraction of the total Ai14^{Mc4r} population (unpaired 2-tailed t test, $t_{(6)}$=4.544, P=0.0039). **g**, Induction of *Mc4r* ISH signal in the VMHvl compared to MEA.

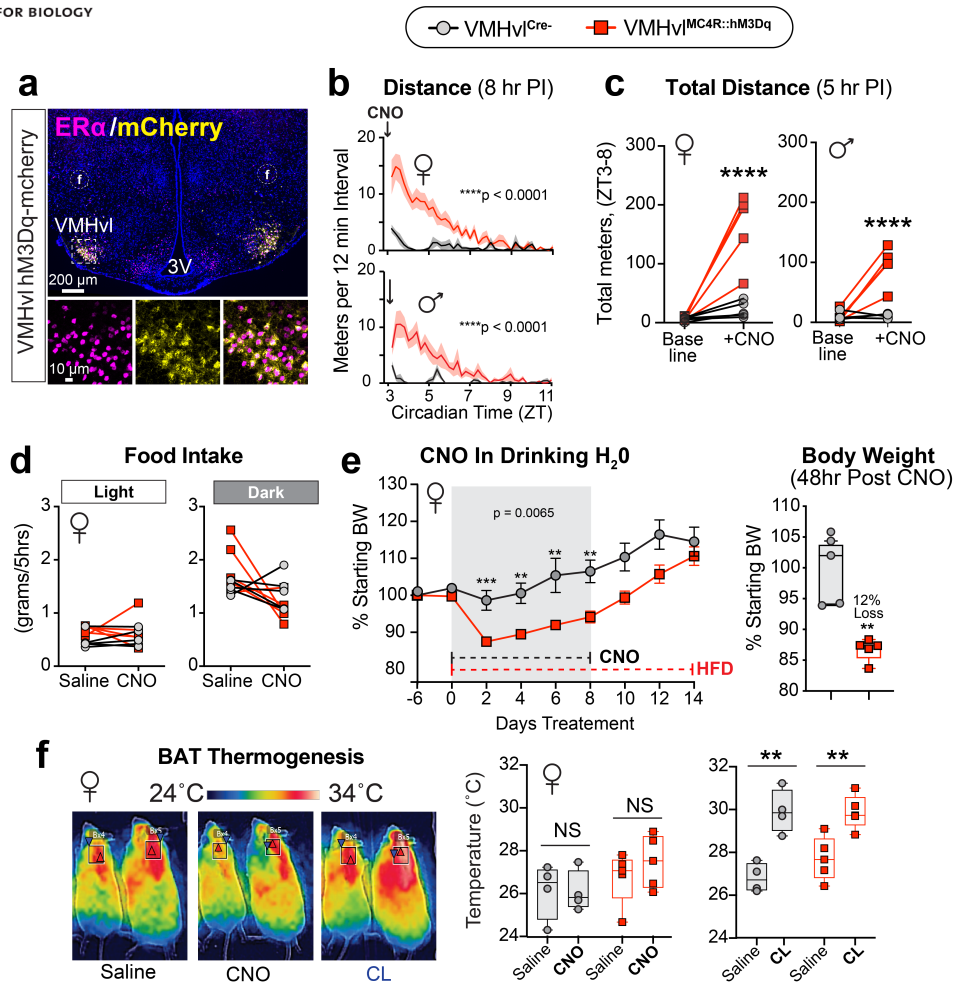

Figure 3. Stimulating VMHvl^{MC4R} neurons promotes energy expenditure by increasing spontaneous physical activity. a, Expression of Cre-dependent AAV-hM3Dq-mCherry restricted to the VMHvl subpopulation in a representative VMHvl$^{MC4R::hM3Dq}$ mouse. **b**, CNO significantly increased locomotor behavior in female and male VMHvl$^{MC4R::hM3Dq}$ mice compared to Cre- littermates (RM 2-way ANOVA: female interaction effect $F_{(39,312)}$=11.96, P<0.0001 and male interaction effect $F_{(39,312)}$=6.898, P<0.0001). **c**, Total distance traveled between ZT3-ZT8 with and without CNO (Baseline) in VMHvl$^{MC4R::hM3Dq}$ and control mice. (RM 2-way ANOVA female interaction effect $F_{(1,8)}$=27.48, P=0.0008, post hoc P<0.0001 and male interaction effect $F_{(1,7)}$=36.27, P=0.0005, post hoc P<0.0001) **d**, Food consumption over a 5 hr period following CNO injection during the light (ZT4) or dark (ZT12) phase. **e**, VMHvl$^{MC4R::hM3Dq}$ females maintained on HFD with chronic chemogenetic stimulation (RM 2-way ANOVA interaction effect $F_{(5,35)}$=4.837, P=0.0018, post hoc: P=0.0010, 0.0088, 0.0014, and 0.0073). Body weights of VMHvl$^{MC4R::hM3Dq}$ mice during the first 48 hrs of CNO exposure (unpaired 2-tailed t test $t_{(8)}$=4.963, P=0.0011). **f**, Thermal imaging of BAT surface temperatures in Cre- control (left) and VMHvl$^{MC4R::hM3Dq}$ (right) females 30min after injection of saline (Sal), CNO (0.3mg/kg), or the β-3 adrenergic agonist, CL-316,243 (CL, 3mg/kg). **g**, Avergage BAT surface temperatures in control and VMHvl$^{MC4R::hM3Dq}$ mice with Saline, CNO and CL. For CL: RM 2-way ANOVA main effect of treatment $F_{(1,7)}$=47.83, P=0.0002, post hoc: Control P=0.0019 and VMHvl$^{MC4R::hM3Dq}$ P=0.0037.

males were sustained during CNO exposure but normalized quickly after withdrawing CNO. In addition to physical activity, a cluster of VMHvl^{ERα} neurons expressing *Rprm* were recently shown to selectively regulate BAT thermogenesis[27]. Despite dramatic changes in activity, we failed to detect CNO-induced changes in BAT temperature (**Fig 3f**) or in other indices of BAT activity (**Extended Data Fig 3.1**), compared to the thermogenic β-3 adrenergic agonist, CL-316,243, (**Fig. 3f**). We noted that baseline BAT temperatures of VMHvl$^{MC4R::hM3Dq}$ females trended higher than controls, likely reflecting an increase in body weights (29.9 ± 2.2 gm vs 24.6 ± 1.3 gm). Overall, these findings pinpoint hormone-sensitive VMHvl^{MC4R} neurons in a potent activity-promoting node that exists in females but can be artificially engaged in males.

To ask if melanocortin signaling itself modulates this VMHvl activity module, we used the reactivatable *Mc4r^{loxTB}* allele[9] to restore *Mc4r* expression on an otherwise null background in VMH neurons. *Sf1-Cre*[28] restored *Mc4r* expression in the VMH, but not in other CNS regions including the PVH (**Fig. 4a**). As expected, by 8 weeks of age, *Mc4r^{loxTB}* null mice gained significantly more weight than control littermates (*Mc4r$^{+/+}$*) (**Fig. 4b and Extended Data Fig 4.1**). Remarkably, despite its absence in the PVH (and elsewhere), restoring *Mc4r* in the VMHvl (*Mc4r$^{Sf1-Cre}$*) substantially attenuated overt obesity in female- but not male-rescued mice.

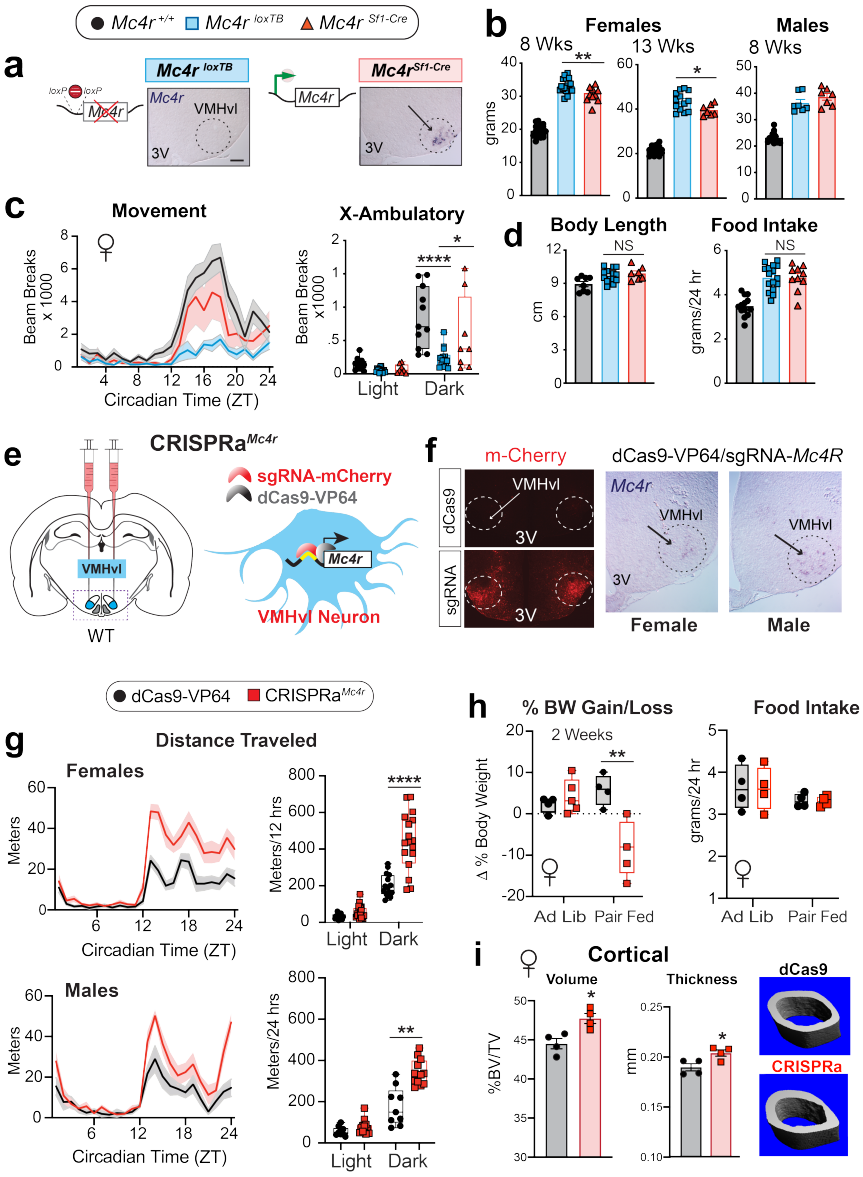

Fig. 4. MC4R Signaling in the VMHvl counteracts profound hyperphagia and drives spontaneous physical activity. a, ISH demonstrating loss of *Mc4r* mRNA in the VMH of *Mc4r*^{loxTB} mice and Sf1-Cre-mediated restoration in *Mc4r*$^{Sf1\text{-}Cre}$ mice. **b**, Female-specific attenuation of obesity in *Mc4r*^{loxTB} mice at 8 weeks of age (1-way ANOVA: female $F_{(2,40)}$=227.7, P<0.0001, post hoc: *Mc4r*$^{+/+}$ vs *Mc4r*^{loxTB} P<0.0001, *Mc4r*$^{+/+}$ vs *Mc4r*$^{Sf1\text{-}Cre}$ P<0.0001, and *Mc4r*$^{Sf1\text{-}Cre}$ vs *Mc4r*^{loxTB} P=0.0117; male $F_{(2,25)}$=92.31, P<0.0001, post hoc: *Mc4r*$^{+/+}$ vs *Mc4r*^{loxTB} P<0.0001, *Mc4r*$^{+/+}$ vs *Mc4r*$^{Sf1\text{-}Cre}$ P<0.0001, and *Mc4r*$^{Sf1\text{-}Cre}$ vs *Mc4r*^{loxTB} P=0.3058). **c**, Dark cycle ambulatory movement in *Mc4r*$^{Sf1\text{-}Cre}$ females to that of *Mc4r*$^{+/+}$, *Mc4r*^{loxTB} mice (RM 2-way ANOVA interaction effect $F_{(2,30)}$=6.4, P=0.0047, post hoc: *Mc4r*$^{+/+}$ vs *Mc4r*^{loxTB} P<0.0001 and *Mc4r*$^{Sf1\text{-}Cre}$ vs *Mc4r*^{loxTB} P=0.0153). **d**, Body-length body length in three cohorts. **e**, Schematic overview of CRISPRa-mediated induction of *Mc4r* via stereotaxic injection into the VMHvl of AAV-dCas9-VP64 and AAV-sgRNA targeting the *Mc4r* promotor. Control mice received dCas9-VP64 alone. **f**, mCherry immunofluorescent staining and *Mc4r* ISH confirmed spatially restricted delivery of the sgRNA and target gene induction, respectively. **g**, Distance traveled for female and male CRISPRa^{Mc4r} mice in home cages over 24 hrs with total distance traveled in light and dark for three top runs (RM 2-way ANOVA female interaction effect $F_{(23,667)}$=4.419, P<0.0001; male interaction effect $F_{(23,437)}$=2.891, P<0.0001). **h**, % body weight change and 24 hr food intake during 2 wk period of ad lib and pair-feeding on standard chow (unpaired 2-tailed t test $t_{(6)}$=3.110, P=0.0208). **i**, Cortical bone volume fraction (unpaired 2-tailed t test, $t_{(6)}$=3.498, P=0.0129) and cortical thickness (unpaired 2-tailed t test, $t_{(6)}$=2.957, P=0.0254) for female cohorts.

Lowered body weights resulted from increased ambulatory movement during the dark phase and not from reduced food intake or from changes in axial lengths; these latter two phenotypes are mediated by melanocortin signaling in the PVH[9].

To verify that Mc4R signaling is an integral component of the hormone-responsive VMHvl activity node, CRISPR-mediated activation (CRISPRa) was employed as previously carried out in the PVH to restore energy balance in haploinsufficient *Mc4r*$^{+/-}$ mice[29]. We injected wild type female and male mice with a dual vector system containing the *Mc4r* promoter guide RNA (*Mc4r*-Pr-sgRNA) and an endonuclease deficient dCas9 tethered to the VP64 transcriptional activator (dCAS9-VP64) to selectively upregulate *Mc4r* expression in the VMHvl (**Fig 4e**). Activity was monitored daily beginning at 7 weeks post-injection. Delivery of *Mc4r*-CRISPRa-viral vectors to the VMHvl and induction of *Mc4r* was confirmed post-mortem (**Fig 4f**). CRISPRa^{Mc4r} females traveled on average two-fold more in the dark phase compared to control females with daily activity persisting at least up to 17 weeks post-injection. In contrast to DREADD-induced movement during the light phase, increased activity was restricted to the dark stage in CRISPRa^{Mc4r} mice suggesting that this manipulation does not disturb normal diurnal activity patterns. Movement in CRISPRa^{Mc4r} males also increased, although as noted with DREADDs above, the total distance traveled by males is lower (Fig 4G). While body weights and food intake were unchanged during ad libitum feeding, pair-feeding resulted in significant loss of body weight over a 2 week period. Daily increase in activity in CRISPRa^{Mc4r} females led to expected increase in cortical bone thickness and volume associated with increased mechanical load (Fig 4H). Other metabolic parameters were unchanged (Extended Data Fig 4.1). Thus,

long-term manipulation of *Mc4r* gene dosage in VMHvl neurons is able to bypass hormone-dependency of this activity node to permanently reduce sedentary behavior.

DISCUSSION

Our findings illustrate how central estrogen signaling in a small subset of VMHvl$^{ERα/MC4R}$ neurons enables episodic bouts of physical activity behaviors, presumably to maximize reproductive success. We show that MC4R is an integral component of an ancillary hormone-responsive exercise node in the female VMHvl that functions independently of MC4R's regulation of satiety. Our data identify the VMHvl as a critical non-PVH site for achieving optimal metabolic health in females and help reconcile the noted sex-differences in the MC4R literature. For example, body weights of *Mc4r*$^{-/-}$ female mice fail to fully normalize upon pair feeding or after restoring *Mc4r* in the PVH/amygdala (via *Sim1-Cre*)[9,16]. Silencing the excitatory output of PVH$^{Sim1/MC4R}$ neurons also led to male but not female obesity prompting the authors to conclude that MC4R actions on other non-SIM1 neurons regulate female energy homeostasis[30]. We speculate that this ancillary estrogen-dependent node is conserved in humans, as women harboring the common *MC4R* SNP (rs17782313) experience greater long-term weight gain, increased risk of diabetes, and emotional eating[31,32].

Although *Mc4r* dosage is critical for proper function and metabolic regulation in both humans and rodent models, endogenous signals that increase its expression have yet to be described. Our data clearly identify estrogen as a potent signal for increasing *Mc4r* expression akin to the gain-of-function human *MC4R* variants that attenuate receptor internalization, which also protect against weight gain[33]. We predict that melanocortin insensitivity in E2-responsive VMHvl neurons partially accounts for the increased sedentary lifestyle associated with estrogen-depletion following menopause[34], while acknowledging that the benefits of estrogen on healthy metabolism likely involve additional MC4R-independent processes[35].

That we are able to bypass hormone-dependent regulation in male VMHvl^{MC4R} neurons to engage this activity node suggests strongly that males possess the same underlying neurocircuitry present in females. Determining whether hormonal surges associated with puberty or social/mating behavior awaken otherwise quiescent VMHvl$^{ERα/MC4R}$ male neurons will be important to address the physiological relevance of this node in males.

Despite the pronounced increased physical activity observed in CRISPRa^{Mc4r} females, lowered body weight was achieved only after restricting food intake. Mice subjected to voluntary exercise and maintained at ambient temperature adjust their metabolism to minimize weight loss[36] mimicking poor outcomes in human weight loss studies that rely solely on exercise[37]. The adaptive basal metabolic responses that prevent the anticipated and sustained weight loss in the face of increased exercise remain to be defined. Regardless, independent of body weight, a sedentary lifestyle represents a significant, modifiable risk factor negatively affecting multiple components of health- and lifespan, including cognition[38,39]. Thus, the higher spontaneous activity observed in CRISPRa^{Mc4r} mice of both sexes in the absence of external environmental pressures (e.g., running wheels) provides a model to explore the motivational aspects and health benefits of an active lifestyle.

Further work aimed at dissecting this hormone-responsive VMHvl activity node in mice and humans will likely provide insights into age-related sedentary behavior and provoke further discussion surrounding hormone replacement therapies in postmenopausal women.

MATERIALS & METHODS

Mice

All experiments were conducted in accordance with UCSF IACUC guidelines and the approved protocol for the Ingraham Lab. *Mc4r*^{loxTB} mice and the *Ai14*$^{fl/fl}$ reporter mice were purchased from Jackson Laboratories and maintained on a C57BL/6J background. *Mc4r*-t2a-*Cre* mice were a generous gift from B. Lowell (BIDMC) and were maintained on a C57BL/6J background. *Esr1*$^{fl/fl}$ were maintained on a mixed background and *Sf1-Cre* mice were maintained on a C57BL/6N in the lab as previously described [3,4].

Wild type mice used for CRISPRa studies were on a pure C57BL/6J background. For *Mc4r* rescue experiments, the *Sf1-Cre* was contributed through female mice. Mice were housed on a 12:12 hour light cycle and had ad libitum access to standard chow (LabDiet #5058) or high-fat diet (Research Diets #D12492). CUT&RUN experiments were performed on adult male (8-12 weeks of age) gonadectomized C57Bl6/J wild type mice obtained from Jackson Laboratory. Three weeks post-gonadectomy, animals were injected subcutaneously with either corn oil (vehicle) or 5 µg of estradiol benzoate and sacrificed after 4 hours. For each biological replicate, brain dissections were pooled from 5 animals.

Stereotaxic Injections

AAV2-Cre-GFP and AAV2-GFP were purchased from the UNC Vector Core (Chapel Hill, NC). AAV2-hM3Dq-mCherry vectors were purchased from Addgene (Watertown, MA). AAVdj-dCas9-VP64 and AAVdj-Prm-Mc4r-sgRNA, were generated by the Stanford Gene Vector and Virus Core and details of vector constructs are as previously described [29],. Adult mice were secured in a Model 1900 stereotaxic frame (David Kopff Instruments), and 250-600 nL of virus was injected bilaterally at the following coordinates: For the VMHvl - A-P: Bregma -1.48 mm, M-L: Bregma +/-0.85 mm, D-V: skull -5.9 mm. For the ARC: A-P: Bregma -1.58 mm, M-L: Bregma +/-0.25 mm, D-V: skull -5.8 mm.

For all surgeries regardless of viral vectors used, mice were allowed to recover for at least 2 weeks prior to any metabolic or behavioral assays. At the conclusion of the experiments, mice

were euthanized and the brains were collected to confirm proper targeting. Any mice absent of fluorescent GFP or mCherry protein expression were excluded from subsequent analyses. Water-soluble CNO (Hello Bio, HB6149) was administered by IP injection (0.3 mg/kg in sterile saline) or in the drinking water (0.25 mg/mL). CNO-laden drinking water was replaced every 48 hours.

Estrous Cycle Staging and EB Treatment

Reproductive stages in female mice were determined by comparing relative amounts of leukocytes, epithelial cells and cornified epithelial cells collected by vaginal lavage. Stage assessments were made daily between ZT3 and ZT5. Brains from estrus or proestrus females were collected between ZT7 and ZT10 and processed for immunofluorescence, ISH, or qPCR.

Adult female mice (>8 week old) were OVX. Estradiol benzoate (Cayman Chemical) was dissolved in DMSO and diluted in sesame oil (Sigma). Mice received subcutaneous injection of either 1ug EB in 150 µL sesame oil or 150 µL of sesame oil with an equivalent amount of DMSO. Control mice received subcutaneous injection of 150 µL of sesame oil with an equivalent amount of DMSO. To minimize changes in VMH gene expression or signal transduction associated with fear/anxiety, mice were handled daily in a manner that simulated injection for at least 5 days prior to EB/Vehicle treatment and tissue collection.

RNA-seq and qPCR

Brains from OVX females treated with EB (n = 4) or vehicle (n = 3) were rapidly dissected into ice-cold PBS with 0.1% DEPC. Coronal brain sections (250 µm thick) were cut on a vibratome and transferred to glass slides so that the VMH could be visualized and manually microdissected. Isolated tissue was flash frozen and stored at -80° C. RNA was prepared using the RNeasy Micro kit (Qiagen). Sequencing libraries were constructed using the TRIO RNA-seq Library Preparation kit (TECAN) using 15 ng of input RNA. Equal amounts of each sample library were multiplexed and sequenced (50 bp single-end reads) on a single flow cell lane HiSeq 4000 (Illumiina). Demultiplexed reads were aligned to the mouse genome (mm10) using HISAT2 [40] and counted using HTSeq [41]. Finally, differential gene expression testing was performed using DESeq2 [42].

Isolated RNA, prepared as described above, was converted to cDNA using the SuperScript III reverse transcriptase (Invitrogen). Target genes were amplified using specific primers (**Extended Data, Table 2**). Ct values were normalized to cyclophilin and relative expression levels were quantified using the comparative C_T method. Individual values, representing the VMHvl from 1 mouse are the average of 2 technical replicates.

CUT&RUN Assay

ERα CUT&RUN was performed on 400,000 nuclei isolated from BNSTp, POA, and MeA tissue via density gradient centrifugation[43]. Briefly, tissue was homogenized 15x with a loose pestle in a glass homogenizer containing Homogenization Medium (250 mM sucrose, 25 mM KCl, 5 mM MgCl2, 20 mM Tricine-KOH, 1 mM DTT, 0.15 mM spermine, 0.5 mM spermidine, 1X Roche EDTA-free protease inhibitor cocktail, pH 7.8). 0.3% IGEPAL CA-630 was added, and the tissue was further dounced 5x with a tight pestle. After douncing, the homogenate was filtered through a 40 µm strainer and mixed 1:1 with 50% OptiPrep solution (Millipore Sigma) prepared in Dilution Buffer (150 mM KCl, 30 mM MgCl2, 120 mM Tricine-KOH, pH 7.8). The homogenate was underlaid with 5 ml of 30% and 40% OptiPrep solution, respectively, and centrifuged at 10,000xg for 18 min at 4°C in an ultracentrifuge. ~2 ml of nuclei solution were removed from the 30 - 40% OptiPrep interface by direct tube puncture. Following nuclei isolation, 0.4% IGEPAL CA-630 was added to improve binding to concanavalin A magnetic beads (Bangs Laboratories BP531). CUT&RUN was performed on brain nuclei, according to the standard protocol [44]. Nuclei were washed twice in Wash Buffer (20 mM HEPES, pH 7.5, 150 mM NaCl, 0.1% BSA, 0.5 mM spermidine, 1X PIC) and incubated overnight on a nutator with ERα antibody (Millipore Sigma 06-935), diluted 1:100 in Antibody Buffer (Wash Buffer containing 2 mM EDTA). Nuclei were washed twice in Wash Buffer, and ~700 ng/ml protein A-MNase (pA-MNase) was added. After 1 hr incubation on a nutator at 4°C, the nuclei were washed twice in Wash Buffer and placed in a metal heat block on ice. pA-MNase digestion was initiated by 2 mM CaCl2. After 90 min, pA-MNase activity was stopped by mixing 1:1 with 2X Stop Buffer (340 mM NaCl, 20 mM EDTA, 4 mM EGTA, 50 µg/ml RNase A, 50 µg/ml glycogen). Digested fragments were released by incubating at 37°C for 10 min, followed by centrifuging at 16,000xg for 5 min at 4°C. DNA was purified from the supernatant by phenol-chloroform extraction.

CUT&RUN Library Preparation

CUT&RUN libraries were prepared using the SMARTer ThruPLEX DNA-seq Kit (Takara Bio), with the following PCR conditions: 72°C for 3 min, 85°C for 2 min, 98°C for 2 min, (98°C for 20 sec, 67°C for 20 sec, 72°C for 30 sec) x 4 cycles, (98°C for 20 sec, 72°C for 15 sec) x 10 cycles. Samples were size-selected with AMPure XP beads (1.5X right-sided and 0.5X left-sided) to remove residual adapter dimers and large DNA fragments. Individually barcoded libraries were multiplexed and sequenced with paired-end 75 bp reads on an Illumina NextSeq, using the High Output Kit.

CUT&RUN Data Processing

Paired-end reads were trimmed to remove low-quality basecalls and adapters. Trimmed reads were aligned to mm10 using Bowtie2 with the following flags: --dovetail --very-sensitive-local --no-unal --no-mixed --no-discordant --phred33 --minins 10 --maxins 700. After alignment, duplicate reads were removed using Picard MarkDuplicates. Subsequently, reads were filtered by mapping quality (MAPQ > 40) and fragment length (< 120 bp). After filtering, peaks were called using MACS2 callpeak with a q-value threshold of 0.05. Filtered BAM files were merged across biological replicates (n = 2) and normalized by counts per million (CPM) for track visualization.

In Situ Hybridization

Antisense *Mc4r* probes were amplified from hypothalamic cDNA libraries (Primer Sequences provided in **Extended Data, Table 2**), and in vitro transcribed with incorporation of digoxigenin-UTP (Roche) using the T7 or SP6 Riboprobe kit (Promega). 20 µm sections from fixed tissue were labeled and detected as previously described [3].

Immunofluorescent Staining

The following antibodies were used for immunofluorescence, polyclonal rabbit anti-ERα (EMD Millipore, #C1355), monoclonal mouse anti-ERα and mouse polyclonal phospho-Serine 244/247 RPS6 (Invitrogen, #44-923G). Alexa Fluor-coupled secondary antibodies (Invitrogen, #A11029 and #A11037).

Metabolic and Activity Monitoring

Indirect calorimetry and food intake were measured in CLAMS chambers (Comprehensive Laboratory Animal Monitoring System, Columbus Instruments). Any spilled food that was not consumed was accounted for at the conclusion of the 4 days period spent in CLAMS.

Ambulatory activity in control and VMHvlMC4R::hM3Dq mice was recorded via IR cameras and quantified using the ANY-maze behavioral tracking system (Stoelting). Prior to any measurements, mice were allowed to acclimate to single-housing in the ANY-maze chambers for at least 1 week. For DREADD studies, control and experimental mice received CNO injections at ZT2.9 and activity tracking began at ZT3. For each mouse, activity parameters were compared to those during the equivalent circadian period on a baseline day in which no CNO was given. For CRISPRa studies, activity tracking was continuously monitored for at least five 24hr periods.
Interscapular skin temperatures was measured using a FLIR-E4 handheld infrared camera (FLIR Systems, Inc. Wilsonville, Oregon) as previously described. Female mice were lightly anesthetized in groups of four or five in an anesthesia induction chamber and images were captured at baseline and 30 minutes post saline, CNO (0.3 mg/kg) or CL-316,243 (3 mg/kg) intraperitoneal injection.

Statistics

Statistical tests, excluding RNA-Seq and CUT&RUN analyses, were performed using Prism 8 (Graphpad). A description of each test and results is provided in the figure legends. Unless otherwise noted, data are presented as mean ± SEM.

Supplementary Information

Extended Data Figure 1.1: VMHvl$^{ER\alpha KO}$ affects brown adipose thermogenesis in mice maintained at ambient temperature.
Extended Data Figure 1.2: VMHvl pS6 induction depends on ERα and can be elicited in males by EB treatment.
Extended Data Figure 2.1: EB-dependent regulation of *Mc4r* and *Nmur2*.
Extended Data 3.1: Chemogenetic activation of VMHvl^{MC4R} neurons reduces sedentary behavior during the normally inactive light period.
Extended Data 3.2: CNO administered in the drinking water stimulates VMHvl^{MC4R} neurons to increase physical activity
Extended Data 4.1: Additional metabolic and expression data for conditional *Mc4r* rescue and CRISPRa^{Mc4r} mice.
Extended Data Table 1: Enriched clusters of estradiol-sensitive DEGs include peptidergic signaling and energy balance regulation.
Extended Data Table 2: Primer sequences used in assays.

ACKNOWLEDGMENTS

We thank Drs. C Paillart and T. McMahon for exceptional technical assistance with the running and data acquisition for the CLAMS and Any-maze systems. Additionally, we thank all members of the Ingraham Lab and Ms. Anne Sufka for their many insightful comments and discussions as well as C. Vaisse for insights on Mc4R signaling. This work was supported by funding to H.A.I. (R01 DK099722, R01AG062331, UCSF Women's Reproductive Health RAP Award, and NRSA NDSP P30- DK097748), to W.C.K. (American Heart Association Postdoctoral Fellowship 16POST27260361), to R.R. (IRACDA K12 GM081266 Program), to B.G. (2T32GM065094), to N.M. (UCSF Mary Ann Koda-Kimble Innovation Seed Award, UCSF Catalyst Program), to S.M.C (K01 DK098320, UCLA Women's Health Center, UL1TR001881), to C.B.H (F32 DK107115-01A1, AHA Postdoctoral Fellowship 16POST29870011) to N.A.(R01 CA197139, R01 MH109907), to J.T. (R01 MH113628, SFARI600568). We wish to acknowledge the mouse metabolic core funded by P30 DK098722-01.

AUTHOR CONTRIBUTIONS

W.C.K. designed experiments, analyzed data and wrote the paper. R.R. performed thermal analysis in mice. B.G. performed Cut&Run experiments. N.M. provided CRISPRa viral vectors and expert advice. A.R. performed histology and quantification of expression data. A.N.P. aided with chemogenetic data acquisition analyses. C.B.H. collected tissues and helped analyzed bone data. S.M.C. designed experiments, provided animal models and analyzed data. N.A. provided key unpublished reagents related to CRISPRa constructs and help guide studies. J. T. optimized Cut&Run method for ERα binding in neurons, performed analyses, wrote and edited manuscript. H.A.I designed experiments, analyzed data, and wrote the manuscript.

REFERENCES

1. Mauvais-Jarvis, F., Clegg, D.J. & Hevener, A.L. The role of estrogens in control of energy balance and glucose homeostasis. *Endocr Rev* **34**, 309-338 (2013).
2. Wade, G.N. Gonadal hormones and behavioral regulation of body weight. *Physiol Behav* **8**, 523-534 (1972).
3. Correa, S.M.*, et al.* An estrogen-responsive module in the ventromedial hypothalamus selectively drives sex-specific activity in females. *Cell Rep* **10**, 62-74 (2015).
4. Herber, C.B.*, et al.* Estrogen signaling in arcuate Kiss1 neurons suppresses a sex-dependent female circuit promoting dense strong bones. *Nat Commun* **10**, 163 (2019).
5. Martinez de Morentin, P.B.*, et al.* Estradiol regulates brown adipose tissue thermogenesis via hypothalamic AMPK. *Cell Metab* **20**, 41-53 (2014).
6. Musatov, S.*, et al.* Silencing of estrogen receptor alpha in the ventromedial nucleus of hypothalamus leads to metabolic syndrome. *Proc Natl Acad Sci U S A* **104**, 2501-2506 (2007).
7. Xu, Y.*, et al.* Distinct hypothalamic neurons mediate estrogenic effects on energy homeostasis and reproduction. *Cell Metab* **14**, 453-465 (2011).
8. Farooqi, I.S.*, et al.* Dominant and recessive inheritance of morbid obesity associated with melanocortin 4 receptor deficiency. *J Clin Invest* **106**, 271-279 (2000).
9. Balthasar, N.*, et al.* Divergence of melanocortin pathways in the control of food intake and energy expenditure. *Cell* **123**, 493-505 (2005).
10. Thammacharoen, S., Lutz, T.A., Geary, N. & Asarian, L. Hindbrain administration of estradiol inhibits feeding and activates estrogen receptor-alpha-expressing cells in the nucleus tractus solitarius of ovariectomized rats. *Endocrinology* **149**, 1609-1617 (2008).
11. Gao, Q.*, et al.* Anorectic estrogen mimics leptin's effect on the rewiring of melanocortin cells and Stat3 signaling in obese animals. *Nat Med* **13**, 89-94 (2007).
12. Cota, D.*, et al.* Hypothalamic mTOR signaling regulates food intake. *Science* **312**, 927-930 (2006).

13. Villanueva, E.C., *et al.* Complex regulation of mammalian target of rapamycin complex 1 in the basomedial hypothalamus by leptin and nutritional status. *Endocrinology* **150**, 4541-4551 (2009).

14. Xu, X., *et al.* Modular genetic control of sexually dimorphic behaviors. *Cell* **148**, 596-607 (2012).

15. Chen, A.S., *et al.* Role of the melanocortin-4 receptor in metabolic rate and food intake in mice. *Transgenic Res* **9**, 145-154 (2000).

16. Ste Marie, L., Miura, G.I., Marsh, D.J., Yagaloff, K. & Palmiter, R.D. A metabolic defect promotes obesity in mice lacking melanocortin-4 receptors. *Proc Natl Acad Sci U S A* **97**, 12339-12344 (2000).

17. Wren, A.M., *et al.* Hypothalamic actions of neuromedin U. *Endocrinology* **143**, 4227-4234 (2002).

18. Skene, P.J. & Henikoff, S. An efficient targeted nuclease strategy for high-resolution mapping of DNA binding sites. *Elife* **6**(2017).

19. Bronstein, R., Gegenhuber, B., Wu, M.V. & Tollkuhn, J. Regulation of gene expression by estrogen receptor alpha in a sexually dimorphic neuronal population. *In Preparation* (2019).

20. Kishi, T., *et al.* Expression of melanocortin 4 receptor mRNA in the central nervous system of the rat. *J Comp Neurol* **457**, 213-235 (2003).

21. Roselli-Rehfuss, L., *et al.* Identification of a receptor for gamma melanotropin and other proopiomelanocortin peptides in the hypothalamus and limbic system. *Proc Natl Acad Sci U S A* **90**, 8856-8860 (1993).

22. Krashes, M.J., Lowell, B.B. & Garfield, A.S. Melanocortin-4 receptor-regulated energy homeostasis. *Nat Neurosci* **19**, 206-219 (2016).

23. Garfield, A.S., *et al.* A neural basis for melanocortin-4 receptor-regulated appetite. *Nat Neurosci* **18**, 863-871 (2015).

24. Pei, H., *et al.* Lateral Hypothalamic Mc3R-Expressing Neurons Modulate Locomotor Activity, Energy Expenditure, and Adiposity in Male Mice. *Endocrinology* **160**, 343-358 (2019).

25. Huszar, D., *et al.* Targeted disruption of the melanocortin-4 receptor results in obesity in mice. *Cell* **88**, 131-141 (1997).

26. Sina, M., *et al.* Phenotypes in three pedigrees with autosomal dominant obesity caused by haploinsufficiency mutations in the melanocortin-4 receptor gene. *Am J Hum Genet* **65**, 1501-1507 (1999).

27. Van Veen, J.E., *et al.* Single cell profiling of the VMH reveals a sexually dimorphic regulatory node of energy expenditure. *BioRxiv* **10.1101/549725**(2019).

28. Dhillon, H., *et al.* Leptin directly activates SF1 neurons in the VMH, and this action by leptin is required for normal body-weight homeostasis. *Neuron* **49**, 191-203 (2006).

29. Matharu, N., *et al.* CRISPR-mediated activation of a promoter or enhancer rescues obesity caused by haploinsufficiency. *Science* **363**(2019).

30. Xu, Y., *et al.* Glutamate mediates the function of melanocortin receptor 4 on Sim1 neurons in body weight regulation. *Cell Metab* **18**, 860-870 (2013).

31. Horstmann, A., *et al.* Common genetic variation near MC4R has a sex-specific impact on human brain structure and eating behavior. *PLoS One* **8**, e74362 (2013).

32. Qi, L., Kraft, P., Hunter, D.J. & Hu, F.B. The common obesity variant near MC4R gene is associated with higher intakes of total energy and dietary fat, weight change and diabetes risk in women. *Hum Mol Genet* **17**, 3502-3508 (2008).

33. Lotta, L.A., *et al.* Human Gain-of-Function MC4R Variants Show Signaling Bias and Protect against Obesity. *Cell* **177**, 597-607 e599 (2019).

34. Lovejoy, J.C., Champagne, C.M., de Jonge, L., Xie, H. & Smith, S.R. Increased visceral fat and decreased energy expenditure during the menopausal transition. *Int J Obes (Lond)* **32**, 949-958 (2008).

35. Xu, P., *et al.* Melanocortin 4 receptor is not required for estrogenic regulations on energy homeostasis and reproduction. *Metabolism* **70**, 152-159 (2017).

36. O'Neal, T.J., Friend, D.M., Guo, J., Hall, K.D. & Kravitz, A.V. Increases in Physical Activity Result in Diminishing Increments in Daily Energy Expenditure in Mice. *Curr Biol* **27**, 423-430 (2017).

37. King, N.A., *et al.* Metabolic and behavioral compensatory responses to exercise interventions: barriers to weight loss. *Obesity (Silver Spring)* **15**, 1373-1383 (2007).

38. Choi, S.H., *et al.* Combined adult neurogenesis and BDNF mimic exercise effects on cognition in an Alzheimer's mouse model. *Science* **361**(2018).

39. DiPietro, L. Physical activity in aging: changes in patterns and their relationship to health and function. *J Gerontol A Biol Sci Med Sci* **56 Spec No 2**, 13-22 (2001).

40. Kim, D., Langmead, B. & Salzberg, S.L. HISAT: a fast spliced aligner with low memory requirements. *Nat Methods* **12**, 357-360 (2015).

41. Anders, S., Pyl, P.T. & Huber, W. HTSeq--a Python framework to work with high-throughput sequencing data. *Bioinformatics* **31**, 166-169 (2015).

42. Love, M.I., Huber, W. & Anders, S. Moderated estimation of fold change and dispersion for RNA-seq data with DESeq2. *Genome Biol* **15**, 550 (2014).

43. Mo, A., *et al.* Epigenomic Signatures of Neuronal Diversity in the Mammalian Brain. *Neuron* **86**, 1369-1384 (2015).

44. Skene, P.J., Henikoff, J.G. & Henikoff, S. Targeted in situ genome-wide profiling with high efficiency for low cell numbers. *Nat Protoc* **13**, 1006-1019 (2018).

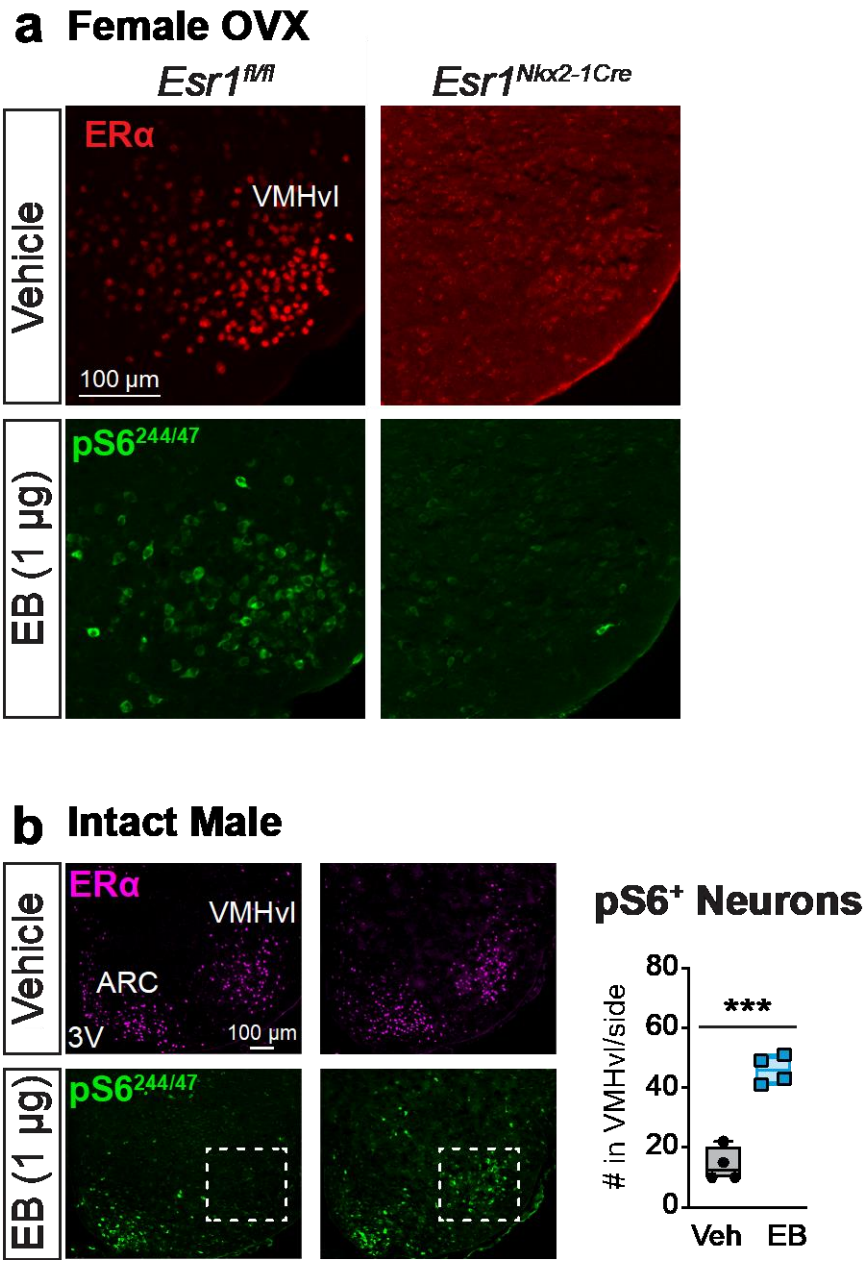

Extended Data Figure 1.1: VMHvl^{ERαKO} affects brown adipose thermogenesis in mice maintained at ambient temperature. a, Equivalent oxygen consumption rates in control, VMHvl^{ERαKO}, and ARC^{ERαKO} female mice measured by indirect calorimetry. **b**, Western blotting for thermogenic UPC1 protein in extracts from control and knockout BAT. **c**, Quantification of the indicated thermogenic gene's expression levels by qPCR.

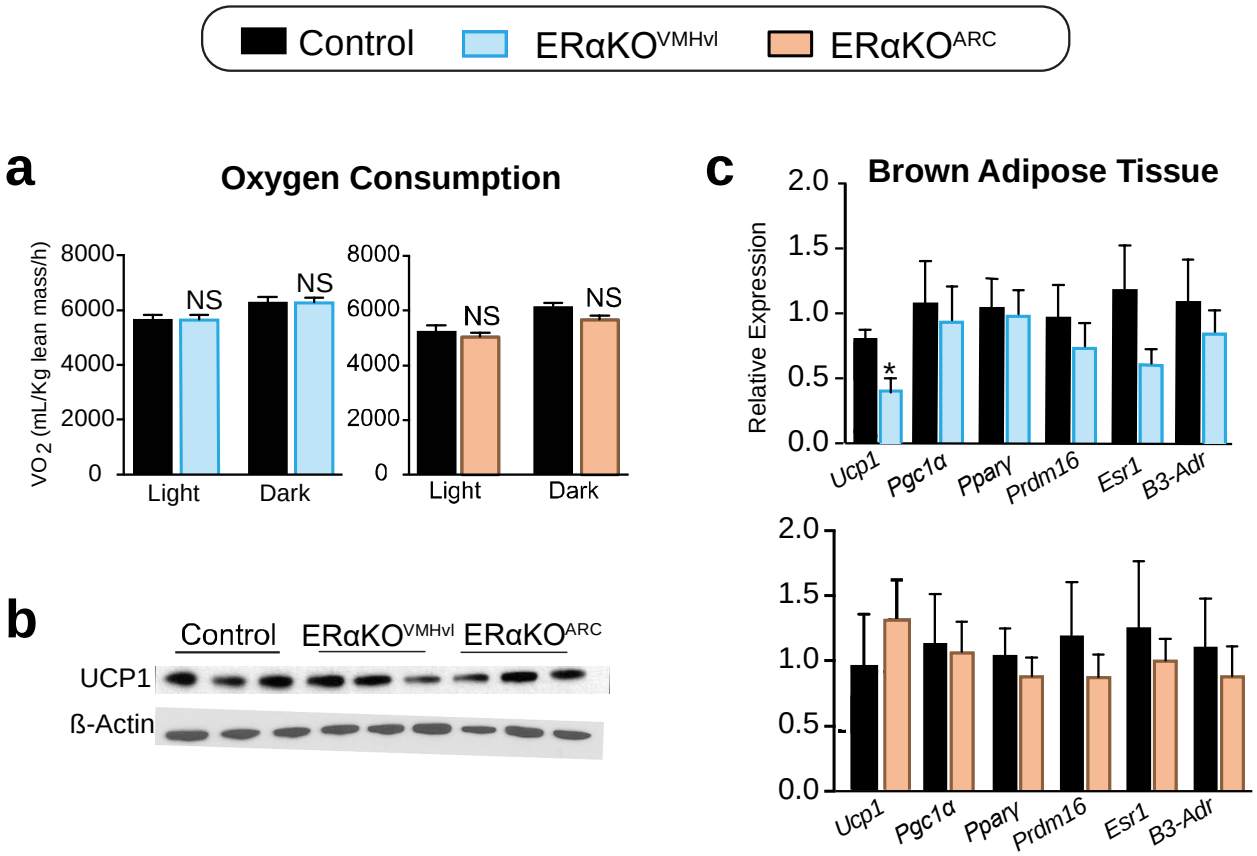

Extended Data Figure 1.2: VMHvl pS6 induction depends on ERα and can be elicited in males by EB treatment. a, Immunofluorescent images of ERα (red) and pS6$^{244/47}$ (green) in the VMHvl of *Esr1*$^{fl/fl}$ and conditional knockout (*Esr1*$^{Nkx2\text{-}1Cre}$) female mice. **b**, EB treatment in male mice increase the number of pS6$^{244/47}$+ neurons in the VMHvl (unpaired 2-tailed *t* test, $t(6)=8.569$, $P=0.0001$).

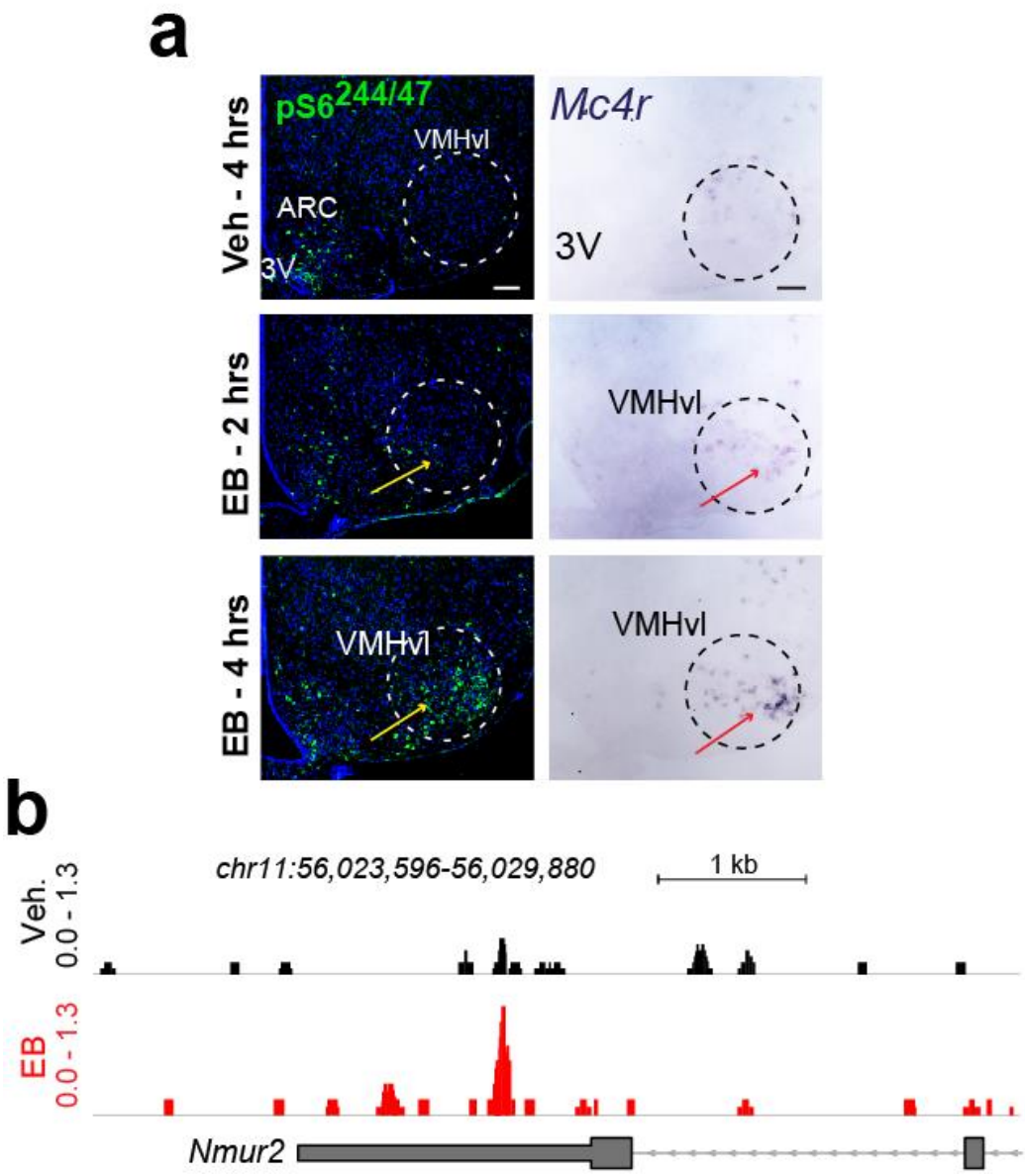

Extended Data Figure 2.1: EB-dependent regulation of *Mc4r* and *Nmur2*. a, Representative immunofluorescent images (pS6) and ISH images (*Mc4r*) in the VMHvl (dashed circle) from OVX female mice treated with vehicle for 4 hrs, EB for 2 hrs, or EB for 4 hrs. **b**, ERα binds to the 3' UTR of Nmur2 in the presence of EB (5 µg).

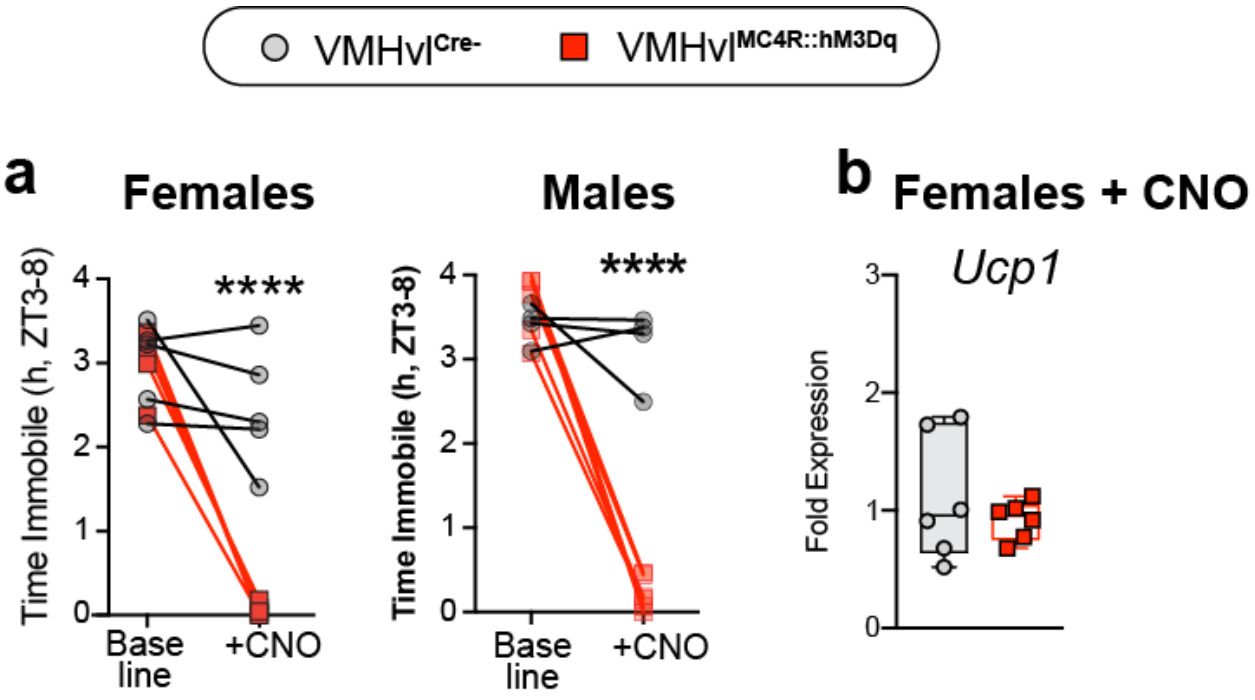

Extended Data 3.1: Chemogenetic activation of VMHvl^{MC4R} neurons reduces sedentary behavior during the normally inactive light period. Quantification of the time spent immobile in female and male VMHvl^{Cre-} controls and VMHvl$^{MC4R::hM3Dq}$ mice (RM 2-way ANOVA female interaction effect $F_{(1,8)}$=33.89, P=0.0004, post hoc P<0.0001 and male interaction effect $F_{(1,8)}$=96.79, P=0.0005, post hoc P<0.0001). Data are from the same ANY-Maze recording sessions as *3b* and *3c*. No differences were observed in BAT *Ucp1* mRNA isolated from the BAT of VMHvl^{Cre-} and VMHvl$^{MC4R::hM3Dq}$ mice collected 1.5 hrs after CNO injection.

Extended Data 3.2: CNO administered in the drinking water stimulates VMHvl^{MC4R} neurons to increase physical activity. Video recording of VMHvl^{Cre-} (left) and VMHvl$^{Mc4r-Cre::hM3dq}$ (right) female mice following addition of CNO-laden drinking water (0.25 mg/mL). Recording has been sped up 20x.

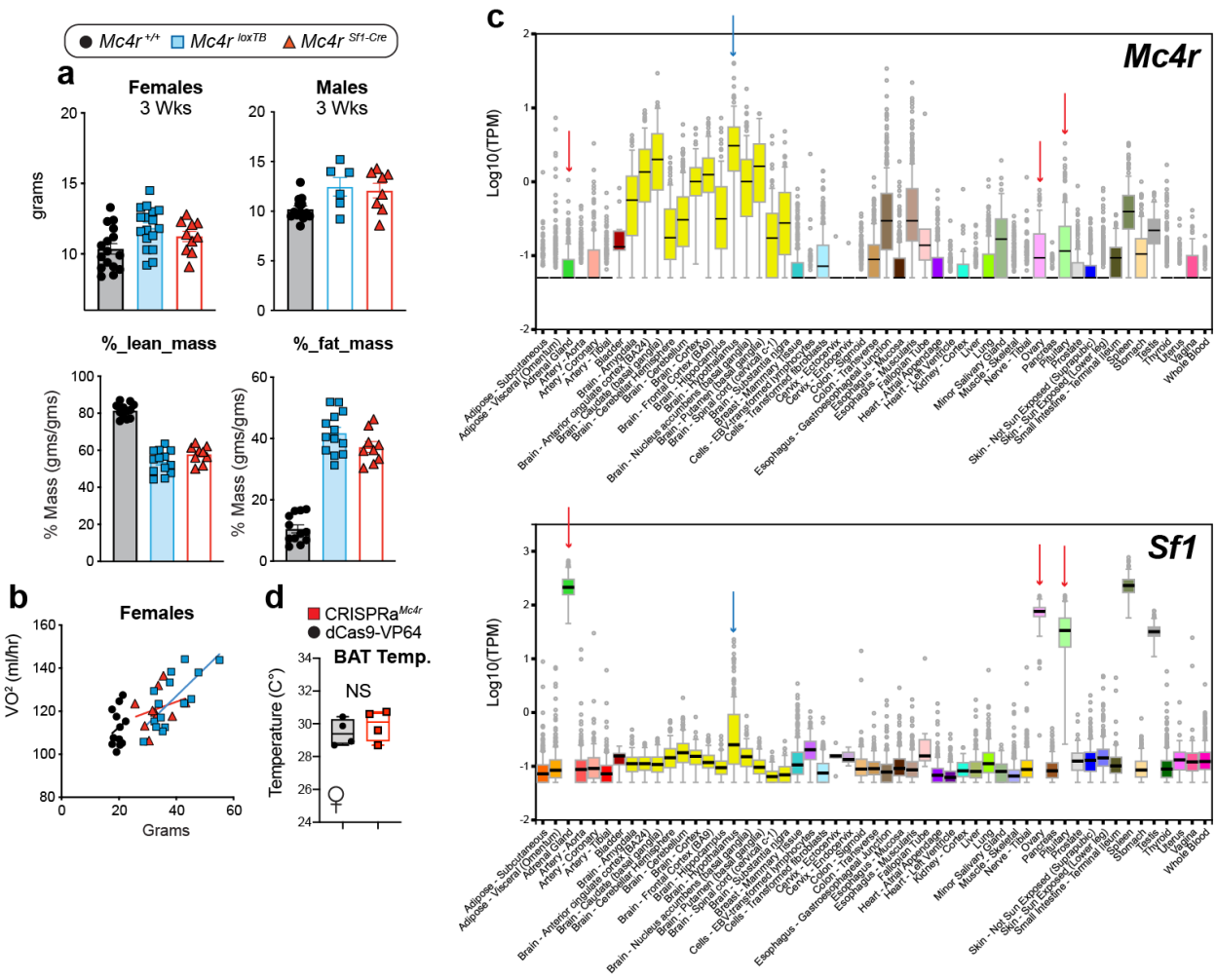

Extended Data 4.1: Additional metabolic and expression data for conditional *Mc4r* rescue and CRISPRa mice. a, Body weights in *Mc4r*$^{+/+}$, *Mc4r*^{loxTB}, and *Mc4r*$^{Sf1\text{-}Cre}$ mice at weaning and body composition analysis (EchoMRI) in adult females of each genotype. **b**, Differences in oxygen consumption (VO2) in adult female *Mc4r*$^{+/+}$, *Mc4r*^{loxTB}, and *Mc4r*$^{Sf1\text{-}Cre}$ mice. **c**, *Mc4r* and *Sf1* expression patterns intersect specifically in the hypothalamus (blue arrows) and not in peripheral tissues (Genotype-Tissue Expression (Gtex) Project data). **d**, No difference in BAT surface temperatures between CRISRPa^{Mc4r} and dCas9-VP64 control female mice.

	Gene	log2 fold change	adjusted P value
Peptide Ligand-Binding Receptors R-MMU-375276	Ackr3	0.57855	0.00994
	Cckar	0.83026	0.00002
	Cckbr	-0.41175	0.04446
	F2r	-0.43494	0.00060
	Mc3r	0.81563	0.00000
	Mc4r	0.93794	0.00000
	Nmur2	0.51415	0.00722
	Npffr1	0.47373	0.04061
	Npy1r	0.75757	0.00000
	Npy4r	0.44735	0.04886
	Oprk1	-0.59674	0.00017
	Oprl1	0.49326	0.00001
	Oprm1	-0.32360	0.04842
	Oxtr	-0.58792	0.00000
	Rxfp3	-0.72515	0.00060
Abnormal Energy Expenditure MP: 0005450	*Arid5b*	-0.40236	0.00124
	Cckbr	-0.41175	0.04446
	Dusp1	0.67125	0.00069
	Ghsr	-0.46711	0.03342
	Gpr12	-0.49815	0.01248
	Lrrc8c	0.94846	0.00000
	Mc3r	0.81563	0.00000
	Mc4r	0.93794	0.00000
	Nmur2	0.51415	0.00722
	Npy1r	0.75757	0.00000
	Tbl1xr1	-0.30377	0.04597
Abnormal Energy Expenditure MP: 0005450	*Arid5b*	-0.40236	0.00124
	Cckar	0.83026	0.00002
	Cckbr	-0.41175	0.04446
	Cftr	0.61554	0.00861
	Dhcr7	0.75968	0.00000
	Ghsr	-0.46711	0.03342
	Irs2	1.09634	0.00000
	Mc3r	0.81563	0.00000
	Mc4r	0.93794	0.00000
	Nmur2	0.51415	0.00722
	Npy1r	0.75757	0.00000
	Npy4r	0.44735	0.04886
	Raph1	0.53286	0.00000
	Sh2d3c	0.42637	0.03811
	Tshz1	-0.37647	0.03109
	Unc5c	-0.47635	0.00001
	Vegfa	0.47349	0.01210

Extended Data Table 1: Enriched clusters of estradiol-sensitive DEGs include peptidergic signaling and energy balance regulation

Target mRNA	Assay	Forward Sequence	Reverse Sequence
Mc4r	qPCR	GCC AGG GTA CCA ACA TGA AG	ATG AAG CAC ACG CAG TAT GG
Nmur2	qPCR	CCTCCTTCCTCTTCTACATCCT	AGTCACTTTGTCTGCCTCAA
Esr1	qPCR	GAACGAGCCCAGCGCCTACG	TCTCGGCCATTCTGGCGTCG
Ppib	qPCR	TGG AGA GCA CCA AGA CAG ACA	TGC CGG AGT CGA CAA TGA T
Mc4r	ISH	ACTCTGGGTGTCATAAGCCTGT	TCTGTCCCCCACTTAATACCTG

Extended Data Table 2: Primer sequences for qPCR and ISH assays